Available online at www.eccomasproceedia.org
Eccomas Proceedia COMPDYN (2025) 682-692

ECCOMAS
Proceedia

COMPDYN 2025
10th ECCOMAS Thematic Conference on
Computational Methods in Structural Dynamics and Earthquake Engineering
M. Papadrakakis, M. Fragiadakis (eds.)
Rhodes Island, Greece, 15-18 June 2025

MULTI-HAZARD FRAGILITY ASSESSMENT OF BRIDGES IN THE MEDITERRANEAN COASTAL REGIONS

M. C. Oddo[1], **L. Cavaleri**[1], **and A. Amato**[1]

[1] University of Palermo
Viale delle Scienze, Ed. 8, Palermo, 90128, Italy
e-mail: {mariaconcetta.oddo01, liborio.cavaleri, anthea.amato}@unipa.it

Abstract

In recent years, growing awareness of the severe threat tsunamis posing to coastal communities has intensified research on their impact, particularly on critical infrastructure such as bridges. While numerous experimental and numerical studies have been conducted to investigate structural vulnerability, analytical assessments remain limited, revealing a significant gap in the literature. Moreover, it is increasingly recognized that coastal regions often experience multi-hazard scenarios, where a tsunami is typically preceded by an earthquake. This sequence heightens structural vulnerability, as seismic damage can substantially reduce the structural capacity to withstand subsequent tsunami forces.

This study introduces a probabilistic multi-hazard fragility assessment framework aimed at evaluating the influence of earthquake-induced damage on the structural response of bridges subjected to sequential tsunami loading. The methodology focuses on bridges with randomly defined geometric and mechanical characteristics representative of those commonly found in Mediterranean coastal areas. Utilizing Monte Carlo simulations, the approach incorporates uncertainties related to tsunami loading, structural configurations, and material properties, enabling a comprehensive and realistic assessment of bridge vulnerability.

Simulation results are used to derive analytical lognormal fragility functions, and a comparative analysis between the numerical data and the fitted distributions confirms the robustness and accuracy of the proposed method. The findings underscore the importance of considering seismic pre-damage in tsunami fragility assessments and demonstrate the potential of the methodology for future applications in multi-hazard risk evaluation.

Keywords: tsunami, tsunami fragility, bridges, multi-hazard, tsunami vulnerability, Monte Carlo simulation.

ISSN:2623-3347
Peer-review under responsibility of the organizing committee of COMPDYN 2025.
doi: 10.7712/120125.12439.25630

1 INTRODUCTION

Bridges are critical infrastructures and key components of the transportation system that effectively combine mobility with the strength of coastal areas. Along the Mediterranean coastlines, for example on the Sicilian coasts, bridges frequently act as crossing arteries for transport and have a strategic importance for the movement of people, commodities, and especially emergency services. Moreover, bridges often serve as escape routes in the aftermath of natural disasters, like earthquakes, landslides, hurricanes, flooding, and tsunamis. For this reason, knowing and preserving their resilience is essential to ensure the effectiveness of the strategic networks, as well as maintaining their structural integrity is fundamental for public safety.

Although tsunami events occur less frequently and with lower intensity in the Mediterranean regions compared to other parts of the world [1], they still pose a serious threat, as historical events have demonstrated. One of the most catastrophic examples is the 1908 tsunami in Messina, which struck the southeastern coast of Sicily, triggering a magnitude 7.2 earthquake and generating waves up to 12 meters high. The total number of victims was approximately 80,000, 2,000 of which produced by only tsunami action [2]. This event also caused severe damage to infrastructures, isolating some parts of the region for an extended period due to the disruption of the connectivity. Based on this experience and damage data from other past post-tsunami events [3], it emerges that the structural reliability of infrastructure against tsunami hazards is crucial for mitigating economic losses in the aftermath of such natural disasters.

Over the last two decades, the scientific community has shown growing interest in studying the effects of tsunami loading on structures and infrastructure [4, 5], using both numerical [6] and experimental approaches [7, 8]. In particular, an increasing number of studies have focused on vulnerability assessment and risk mitigation [9-11], often through the development of fragility curves. Karafagka et al. [4] developed analytical tsunami fragility functions for representative types of seaport structures in Greece using nonlinear static tsunami analyses. Petrone et al. [12] evaluated various analytical methods, including both nonlinear static and nonlinear dynamic analyses, to construct tsunami fragility curves for Reinforced Concrete (RC) structures. More advanced tsunami fragility analyses also account for the effects of preceding earthquake damage through the adoption of innovative multi-hazard approaches. As highlighted in a global review [13] of tsunami events from 1900 to 2020, tsunamis are often triggered by other natural hazards. Globally, earthquakes are the leading cause of tsunamis (80%), followed by landslides (12%) and volcanic activity (5%). On this background, several studies have focused on assessing the tsunami fragility of structures and infrastructure under sequential earthquake-tsunami loading [14,15], reflecting the growing research interest in multi-hazard analysis.

In the present study, a probabilistic multi-hazard framework based on a Monte Carlo simulation approach is introduced to evaluate the tsunami fragility of individual structural elements comprising bridges typical of the Mediterranean coastal regions. The methodology allows for the consideration of damage induced by prior earthquake loading on the structural performance of RC piles under sequential tsunami action, following the two-phase damage analysis approach proposed by Xu et al. [16].

The results are presented in terms of cumulative distribution functions, highlighting the effects of prior earthquake damage on the post-event tsunami performance of bridges. The main aim is to raise awareness of the consequences of combined earthquake–tsunami impacts on coastal areas and to support more effective risk management strategies against these two combined hazards.

2 MULTI-HAZARD FRAMEWORK

The proposed multi-hazard framework is based on Monte Carlo simulation with random inputs, including the randomization of the structural geometries and tsunami parameters. The methodology involves generating a random bridge model and subjecting it to two sequential analyses: a nonlinear Time History Analysis (THA) to simulate earthquake loading, followed by a Push-Over Analysis (POA) to represent tsunami loading. By performing these analyses in sequence, the methodology captures the realistic tsunami fragility of bridges. This is crucial because tsunamis are often triggered by preceding earthquakes [13], which can cause initial damage to the bridge due to dynamic loading. As a result, the structural capacity of the bridge may be reduced before the tsunami forces act on its elements, leading to an accumulation of damage that compromises its overall performance during the tsunami event.

To ensure the integrity of the stochastic process and optimize computational efficiency, the entire multi-hazard framework is implemented in Python [17], utilizing the OpenSeesPy library [18] for structural analysis. OpenSeesPy is a Python-based interface for the open-source Finite Element (FE) platform OpenSees.

The procedure begins by generating a bridge model with random geometrical properties. Its structural response to earthquake excitation is then evaluated through the THA, using a spectrum-compatible accelerogram characterized by a specific value of the Peak Ground Acceleration (PGA) representative of the seismic conditions typical of Mediterranean regions. If the model collapses during THA, the process skips the POA and restarts by generating a new random bridge model with different geometric characteristics and repeating the THA. If the model withstands the earthquake, the analysis proceeds with the POA to evaluate the performance of the damaged model under various possible subsequent tsunami loading conditions. At this stage, to account for the stochastic nature of tsunami events, random pairs of inundation depth (h) and flow velocity (v) are generated, as detailed in the following.

In this study, the tsunami fragility is evaluated by considering collapse as the damage state. Each time the POA fails, i.e. the structural model reaches its maximum capacity, the corresponding value of h that led to collapse is recorded in a count vector.

At the end of the Monte Carlo simulations, the collected data are post-processed to first determine the fragility points and then calculate the statistical parameters: the mean (μ) and standard deviation (β). These statistical values are calculated considering the logarithms of the h values, as analytical fragility curves are finally plotted assuming a lognormal distribution, which provides a reliable representation of the probability of collapse under tsunami loading [19].

2.1 Numerical models

The combined time history and push-over analyses (THA-POA) were performed on bridge models with randomly generated geometrical characteristics. Specifically, 20 models were generated based on the scheme shown in Figure 1. Uniform distributions were assumed for the random parameters: h_p (column height), D (diameter of the circular columns), L (span length), B (deck width), and t (deck thickness), within the ranges specified in Table 1.

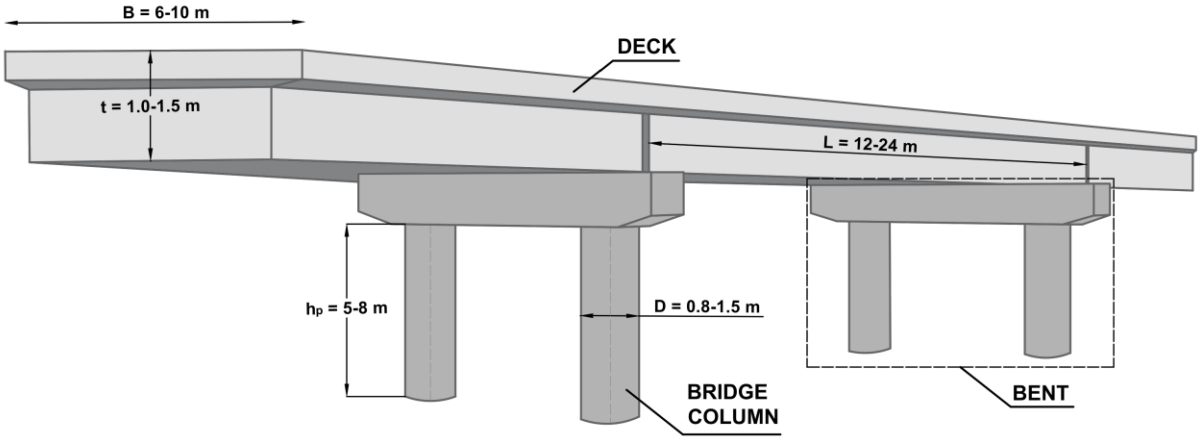

Figure 1: General layout for bridge models.

	Random Variable	Distribution	Range
Geometric variables	h_p	Uniform	5-8 m
	D		0.8-1.5 m
	L		12-24 m
	B		6-10 m
	t		1.0-1.5 m

Table 1: Assumed distributions for geometric characteristics.

In the present study, the performance and vulnerability of bridge structures were evaluated by analyzing the response of individual two-column bents subjected to sequential earthquake and tsunami loading. These bents were modeled as simple frames consisting of two columns connected by a rigid beam, as illustrated in Figure 2, with the vertical load (P_{load}) concentrated at the top of the columns. Each column was modeled using a fiber-based nonlinear beam-column element, with the mass (m) assumed to be concentrated at the top node (Node j).

Simplified boundary conditions were adopted for this preliminary study. The base of each column (Node i) was assumed to be fixed, neglecting soil-structure interaction - despite its significant influence, particularly under horizontal loading - while the top of the frame (Node j) was left free to translate and rotate.

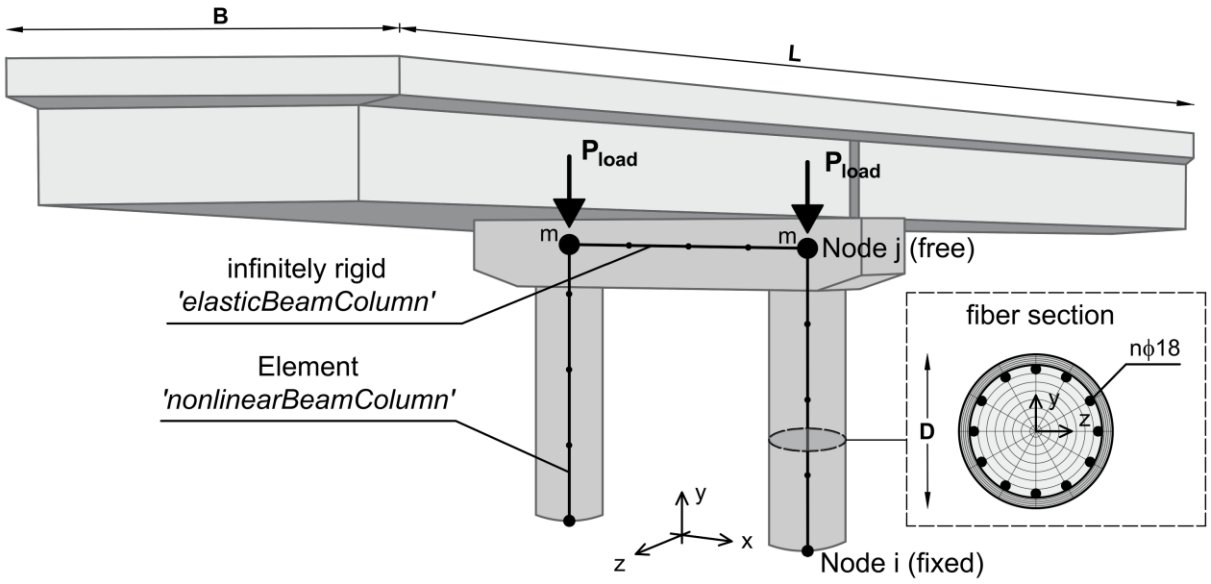

Figure 2: Fiber-section based model for two-column bent.

The reinforced concrete fiber section was modeled using the 'Steel02' uniaxial material for the steel fibers, and 'Concrete02' uniaxial material for both the concrete cover (unconfined concrete) and the concrete core. The main parameters defining these materials are summarized in Table 2.

Steel02		Concrete02	unconfined	confined
f_y	391 MPa	f_{pc}	30 MPa	39 MPa
E_0	210 GPa	eps_{c0}	0.002	0.0025
b	0.01	f_{pcu}	6 MPa	7.8 MPa
R0	15	eps_U	0.0035	0.025
cR1	0.925	lambda	0.1	0.1
cR2	0.15	f_t	4 MPa	5 MPa
		E_{ts}	27 GPa	31 GPa

Table 2: Parameters assumed for Steel02 and Concrete02 material constitutive models.

2.2 Nonlinear time-history analysis

Nonlinear time history analysis (THA) was performed to simulate the earthquake loading preceding the tsunami events. In this study, 20 randomly generated bridge models were subjected to three different levels of ground motion intensity, using spectrum-compatible accelerograms characterized by Peak Ground Acceleration (PGA) values of 0.15g, 0.25g, and 0.50g (Figure 3a). The selected ground motions were applied in the transverse direction of the bridge (x-direction), as shown in Figure 3b, to assess the severity of the induced damage. At the end of the dynamic analysis, if the model withstood the earthquake loading, its resulting damage state was preserved and used as the initial condition for the subsequent Push-Over Analysis (POA).

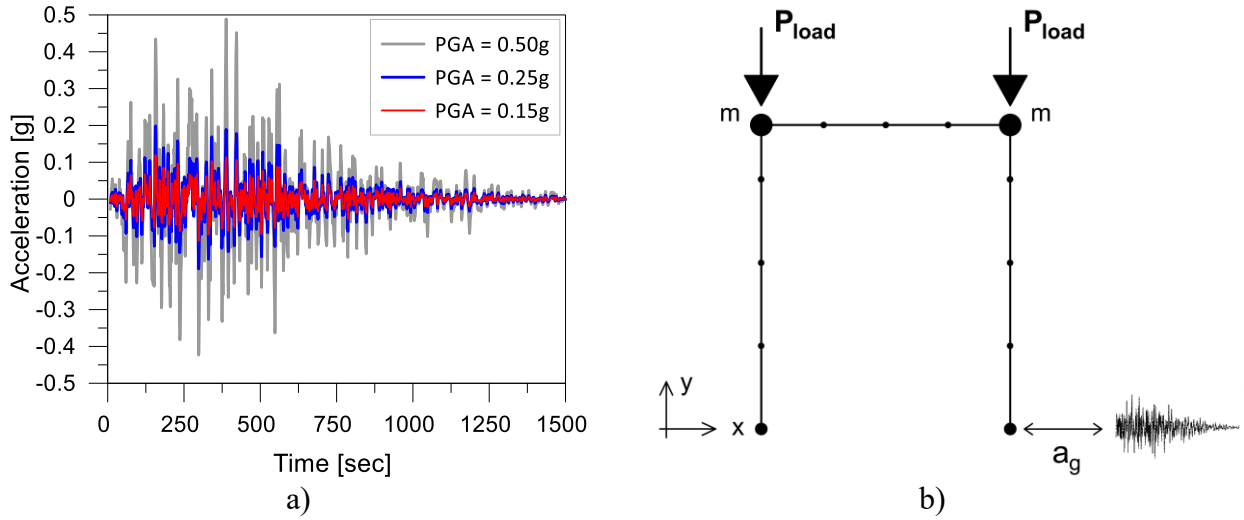

Figure 3: Time History Analysis (THA) of the bridge under earthquake loading: (a) spectrum-compatible accelerograms; (b) bridge bent configuration with no damage.

2.3 Tsunami push-over analysis

At the end of the dynamic analysis (THA), the post-earthquake damage state was kept and used as the initial condition for the second stage of the simulation (POA). The second phase consisted in performing a series of force-controlled POA to simulate the effects of tsunami loading on the pre-shocked bridge bent model (Figure 4).

In real scenarios, tsunami-induced forces on structures arise from a combination of actions that may occur simultaneously or sequentially. These include hydrostatic forces (F_h), buoyant forces, hydrodynamic forces (F_d), impulsive forces (F_i), debris impact, debris damming, and uplift forces. However, to simplify the analysis in this study, only the dominant effect associated with the hydrodynamic force (F_d) was considered, as shown in Figure 4b, and it was calculated using Equation (1) according to FEMA P-646 [20]:

$$F_d = \frac{1}{2} \cdot \rho \cdot D \cdot C_D \cdot (h \cdot v^2) \tag{1}$$

where ρ is the fluid density including the sediments (1100 kg/m^3), g is the gravitational acceleration, D is the diameter of the column impacted by the flow, and C_D is the drag coefficient assumed equal to 1.1.

The uncertainties associated with tsunami actions were included in the analysis by generating random values of the flow velocity (v) corresponding to each inundation depth value (h). Specifically, inundation depths ranged from 0.5 m to 9.0 m, with increments of 0.50 m. For each inundation depth value, 100 random velocity values were generated, assuming a uniform probability distribution. The velocity values were selected within a range defined by the minimum (v_{min}) and the maximum velocity (v_{max}) values, calculated based on the Froude number (F_r). In detail, the Froude number was assumed to be 0.7 for the lower bound and 2.0 for the upper bound (Figure 4a), based on field data and theoretical observations available in [21]. Accordingly, v_{min} and v_{max} were calculated with the following Equations (2) and (3), respectively:

$$v_{min} = 0.7 \cdot \sqrt{g \cdot h} \tag{2}$$

$$v_{max} = 2.0 \cdot \sqrt{g \cdot h} \tag{3}$$

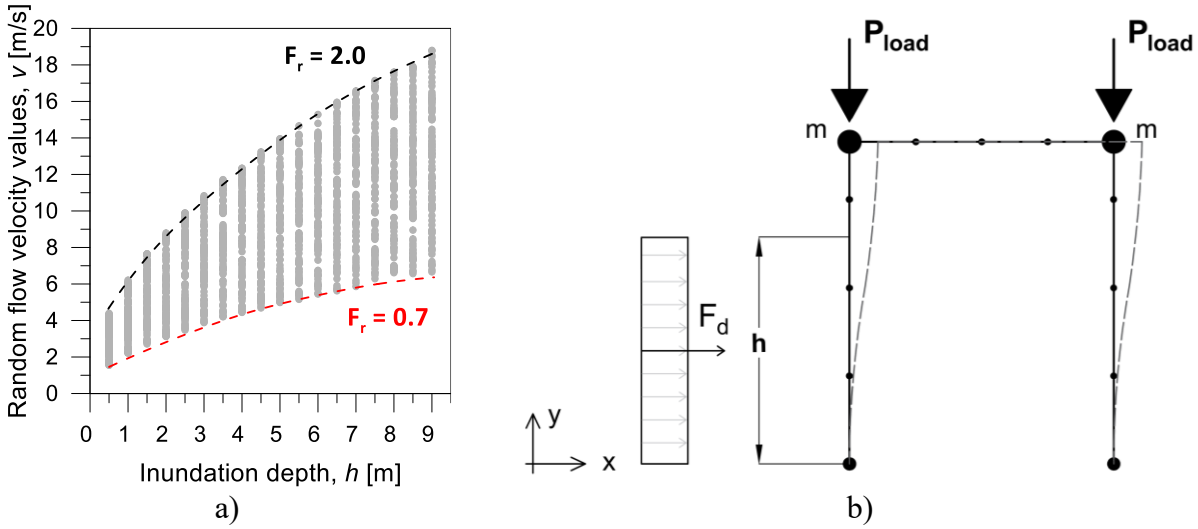

Figure 4: Push-Over Analysis (POA) of the bridge under tsunami loading: (a) random flow velocity values coupled with inundation depths; (b) post-earthquake-damaged bridge bent model.

3 MULTI-HAZARD FRAGILITY FUNCTIONS

Using the Monte Carlo simulation approach outlined in the previous section, fragility curves were obtained for varying levels of seismic intensity: no earthquake, and Peak Ground Acceleration (PGA) values of 0.15g, 0.25g, and 0.50g.

Upon completing the Monte Carlo simulations, a dataset of numerical fragility points was obtained, enabling the estimation of collapse probabilities at various inundation depths. Assuming a lognormal distribution for fragility, the mean (μ) and standard deviation (β) of the logarithms of the inundation depths that led to collapse were calculated. These two statistical parameters were used to construct the probability density function *f(h)*, according to Equation 4, which includes all collapse cases resulting from both prior seismic loading and subsequent tsunami loading.

$$f(h) = \frac{1}{h\,\beta\,\sqrt{2\pi}} \exp\left(-\frac{(\ln h - \mu)^2}{2\beta^2}\right) \tag{4}$$

Then, to account for the percentage of models that failed due to seismic loading alone, the analytical probability density function *f(h)* was adjusted by applying a horizontal shift equal to $\bar{h}$, as illustrated in Figure 5.

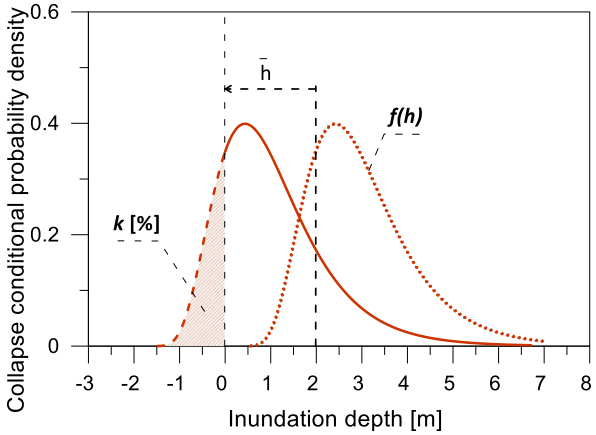

Figure 5: Shift of the conditional probability density function to account for seismic-induced collapse.

Begin the value $\bar{h}$ obtained by solving the following integral:

$$\int_0^{\bar{h}} f(h)dh = k \tag{5}$$

In this integral (Equation 5), the parameter k denotes the percentage of models that collapsed under earthquake loading alone, as determined from the Monte Carlo simulation results.

As a result, the final analytical fragility function $F(h)$ is derived from the well-known cumulative lognormal distribution function, modified as follows:

$$F(h) = k + (1 - k) \cdot \Phi\left(\frac{\ln h - \mu}{\beta}\right) \tag{6}$$

where Φ represents the cumulative distribution function of the standard normal distribution.

4 RESULTS AND COMPARISONS

The results obtained from the Monte Carlo simulations, following the procedure described above, were compared with the analytical fragility curves defined by the statistical parameters μ, β, and k. As shown in Figure 6, these comparisons were conducted for bridge bent models subjected to different levels of earthquake intensity (no earthquake, PGA = 0.15g, PGA = 0.25g, and PGA = 0.50g). The results indicate that the trend of the fragility points obtained from the simulations align with good approximation with the lognormal cumulative distribution functions, validating the accuracy of the analytical fragility model.

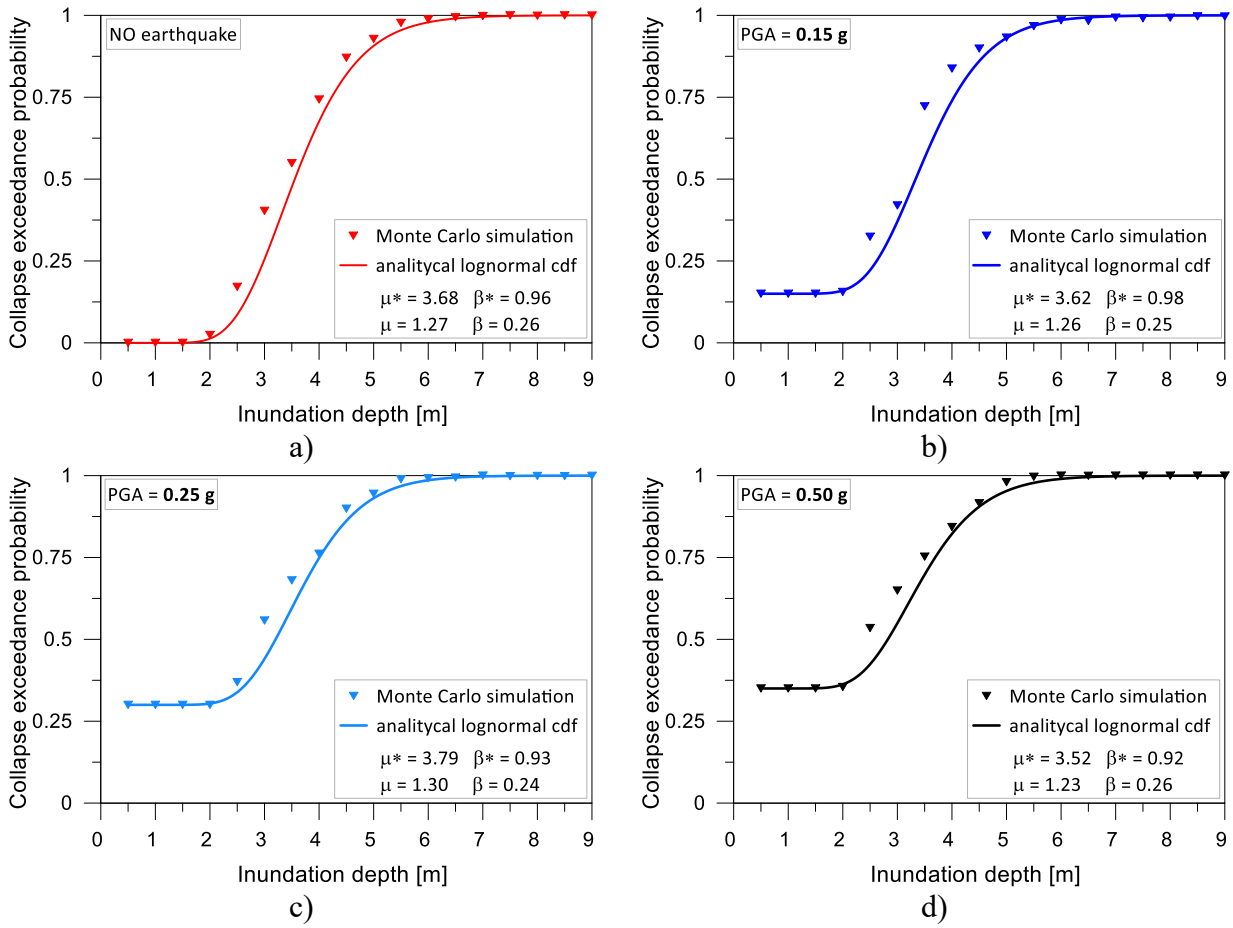

Figure 6: Multi-hazard fragility curves: a) no earthquake; b) PGA = 0.15g; c) PGA = 0.25g; d) PGA = 0. 50g.

Each fragility curve exhibits a characteristic horizontal plateau at lower inundation depths. This plateau represents the probability of collapse induced by seismic loading alone, before any tsunami effects occur. As expected, the height of this plateau increases by increasing the earthquake intensity. For example, at PGA = 0.15g, approximately 15% of the models collapsed due to seismic action alone, while this percentage rises to 35% at PGA = 0.50g.

This trend reflects the impact of seismic pre-damage on structural vulnerability: as ground motion intensity increases, the columns experience a greater stiffness degradation and loss of capacity, making them more susceptible to subsequent tsunami forces. Consequently, the tsunami-induced inundation depth required to achieve the collapse decreases with higher PGA levels.

These observations are further illustrated in Figure 7, which presents both the analytical fragility curves at different seismic intensity levels (Figure 7a) and the corresponding multi-hazard fragility surface (Figure 7b). The 3D surface in Figure 7b shows the probability of collapse as a function of both earthquake intensity (PGA) and tsunami inundation depth. The plots show how increasing seismic intensity reduces the inundation depth required to achieve the structural collapse. This highlights the compounding effects of sequential hazards and emphasizes the importance of accounting for earthquake-induced damage in tsunami fragility assessments.

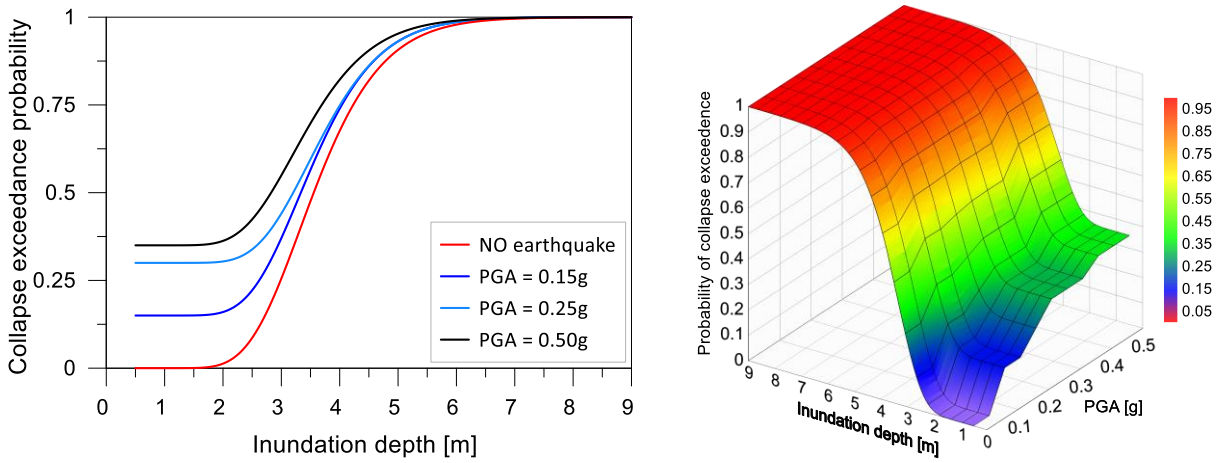

Figure 7: Multi-hazard tsunami fragility curves: a) analytical collapse exceedance probability at various inundation depths and prior earthquake intensity levels; b) interaction surface of prior earthquake intensity and post-shock tsunami inundation depth.

5 CONCLUSIONS

This study introduces a simplified framework for the development of multi-hazard fragility curves, aimed at evaluating the tsunami-induced vulnerability of bridges that have been pre-damaged by seismic events. The methodology, based on Monte Carlo simulations, is here applied to simplified single bent bridge models with fixed-base constraints. In this preliminary investigation, the tsunami loading was represented exclusively by hydrodynamic forces, and other tsunami effects were neglected.

The results provide that:

- earthquake-induced damage in bridge bents, when not leading to immediate collapse, significantly reduces structural stiffness and load-carrying capacity;

- increasing earthquake intensity (PGA) leads to greater pre-damage, lowering the threshold inundation depth required to cause the collapse under tsunami loads;
- ignoring prior seismic damage may result in a considerable underestimation of structural vulnerability in combined earthquake-tsunami scenarios.

While this study provides valuable insights, it also highlights the need for further research to improve the robustness and realism of multi-hazard fragility models. Specifically, future studies should incorporate:

- additional tsunami-induced forces, such as the vertical buoyancy, which can significantly affect structural performance - especially when the tsunami inundation depth reaches the height of the bridge deck;
- a detailed soil-structure interaction, which plays a critical role in presence of horizontal forces;
- other bridge typology can be included in the analysis, which may experience different failure modes and interact differently with tsunami flows.

ACKNOWLEDGMENTS

This study was carried out within the RETURN Extended Partnership and received funding from the European Union Next-Generation EU (National Recovery and Resilience Plan – NRRP, Mission 4, Component 2, Investment 1.3 – D.D. 1243 2/8/2022, PE0000005).

REFERENCES

[1] National Geophysical Data Center / World Data Service: NCEI/WDS Global Historical Tsunami Database. NOAA National Centers for Environmental Information. doi:10.7289/V5PN93H7.

[2] S. Tinti and A. Armigliato, Impact of large tsunamis in the Messina Straits, Italy: the case of the 28 December 1908 tsunami. In *Tsunami Research at the End of a Critical Decade* (pp. 139-162). Dordrecht: Springer Netherlands, 2001.

[3] Headquarters EDC. Damage situation and police countermeasures associated with 2011 Tohoku district-off the Pacific Ocean earthquake. *National Police Agency of Japan,* Tokyo, 2016.

[4] S. Karafagka, S. Fotopoulou and K. Pitilakis, Analytical tsunami fragility curves for seaport RC buildings and steel light frame warehouses. Soil Dynamics and Earthquake Engineering, 112, 118-137, 2018.

[5] J. Rahman and A. M. Billah, Vulnerability Assessment of Coastal Bridges Subjected to Tsunami Loading. *Canadian-Pacific Conference on Earthquake Engineerin*, Vancouver, June 2023.

[6] L. Cavaleri, G. Ciraolo, M. F. Ferrotto, G. La Loggia, C. L. Re, G. Manno, Masonry structures subjected to tsunami loads: modeling issues and application to a case study. In *Structures* (Vol. 27, pp. 2192-2207). Elsevier, 2020.

[7] B. Seiffert, M. Hayatdavoodi, R. C. Ertekin, Experiments and computations of solitary-wave forces on a coastal-bridge deck. Part I: Flat plate. *Coastal Engineering*, 88, 194-209, 2014.

[8] M. Hayatdavoodi, B. Seiffert, R. C. Ertekin, Experiments and computations of solitary-wave forces on a coastal-bridge deck. Part II: Deck with girders. *Coastal Engineering*, 88, 210-228, 2014.

[9] A. Suppasri, P. Latcharote, J. D. Bricker, N. Leelawat, A. Hayashi, K. Yamashita, ... F. Imamura, Improvement of tsunami countermeasures based on lessons from The 2011 Great East Japan Earthquake and Tsunami—situation after five years. *Coastal Engineering Journal*, 58(04), 1640011, 2016.

[10] N. Horspool, I. Pranantyo, J. Griffin, H. Latief, D. H. Natawidjaja, W. Kongko, ... H. K. Thio, A probabilistic tsunami hazard assessment for Indonesia. *Natural Hazards and Earth System Sciences*, 14(11), 3105-3122, 2014.

[11] J. Macabuag, and T. Rossetto, Towards the development of a method for generating analytical tsunami fragility functions. In *2nd European conference on earthquake engineering and seismology*, 2014.

[12] C. Petrone, T. Rossetto, K. Goda, Fragility assessment of a RC structure under tsunami actions via nonlinear static and dynamic analyses. *Engineering Structures*, 136, 36-53, 2017.

[13] J. A. Reid and W. D. Mooney, Tsunami occurrence 1900–2020: A global review, with examples from Indonesia. *Pure and Applied Geophysics*, 180(5), 1549-1571, 2023.

[14] S. Park, J. W. van de Lindt, D. Cox, R. Gupta, F. Aguiniga, Successive earthquake-tsunami analysis to develop collapse fragilities. *Journal of Earthquake Engineering*, 16(6), 851-863, 2012.

[15] C. Petrone, T. Rossetto, M. Baiguera, C. De la Barra Bustamante, I. Ioannou, Fragility functions for a reinforced concrete structure subjected to earthquake and tsunami in sequence. *Engineering Structures*, 205, 110120, 2020.

[16] J. G. Xu, G. Wu, D. C. Feng, J. J. Fan, Probabilistic multi-hazard fragility analysis of RC bridges under earthquake-tsunami sequential events. *Engineering Structures*, 238, 112250, 2021.

[17] F. McKenna, OpenSees: a framework for earthquake engineering simulation. *Computing in Science & Engineering*, 13(4), 58-66, 2011.

[18] M. Zhu, F. McKenna, M. H. Scott, OpenSeesPy: Python library for the OpenSees finite element framework. *SoftwareX*, 7, 6-11, 2018.

[19] M. C. Oddo, P. G. Asteris, L. Cavaleri, Monte Carlo analysis of masonry structures under tsunami action: reliability of lognormal fragility curves and overall uncertainty prediction. In *Structures* (Vol. 63, p. 106421), Elsevier, 2024.

[20] FEMA, Guidelines for Design of Structures for Vertical Evacuation from Tsunamis. (FEMA P-646). *FEMA P-646 Publ*, 2012.

[21] H. Matsutomi and K. Okamoto, Inundation flow velocity of tsunami on land. Island Arc, 19(3), 443-457, 2010.